

RESEARCH PAPER

Physiological and genetic analysis of CO₂-induced breakdown of self-incompatibility in *Brassica rapa*

Xintian Lao¹, Keita Suwabe², Satoshi Niikura³, Mitsuru Kakita¹, Megumi Iwano¹ and Seiji Takayama^{1,*}

¹ Graduate School of Biological Sciences, Nara Institute of Science and Technology, Ikoma, Nara 630-0192, Japan

² Graduate School of Bioresources, Mie University, Tsu 514-8507, Japan

³ Tohoku Seed Co. Ltd, Utsunomiya 321-3232, Japan

* To whom correspondence should be addressed. E-mail: takayama@bs.naist.jp

Received 17 July 2013; Revised 18 November 2013; Accepted 21 November 2013

Abstract

Self-incompatibility (SI) of the Brassicaceae family can be overcome by CO₂ gas treatment. This method has been used for decades as an effective means to obtain a large amount of inbred seeds which can then be used for F₁ hybrid seed production; however, the molecular mechanism by which CO₂ alters the SI pathway has not been elucidated. In this study, to obtain new insights into the mechanism of CO₂-induced SI breakdown, the focus was on two inbred lines of *Brassica rapa* (syn. *campestris*) with different CO₂ sensitivity. Physiological examination using X-ray microanalysis suggested that SI breakdown in the CO₂-sensitive line was accompanied by a significant accumulation of calcium at the pollen–stigma interface. Pre-treatment of pollen or pistil with CO₂ gas before pollination showed no effect on the SI reaction, suggesting that some physiological process after pollination is necessary for SI to be overcome. Genetic analyses using F₁ progeny of a CO₂-sensitive × CO₂-insensitive cross suggested that CO₂ sensitivity is a semi-dominant trait in these lines. Analysis of F₂ progeny suggested that CO₂ sensitivity could be a quantitative trait, which is controlled by more than one gene. Quantitative trait locus (QTL) analyses identified two major loci, *BrSIO1* and *BrSIO2*, which work additively in overcoming SI during CO₂ treatment. No QTL was detected at the loci previously shown to affect SI stability, suggesting that CO₂ sensitivity is determined by novel genes. The QTL data presented here should be useful for determining the responsible genes, and for the marker-assisted selection of desirable parental lines with stable but CO₂-sensitive SI in F₁ hybrid breeding.

Key words: *Brassica rapa*, calcium, CO₂, F₁ hybrid, QTL, self-incompatibility.

Introduction

Self-incompatibility (SI) is a widespread genetic system in many flowering plants which serves to prevent self-fertilization and maintain genetic diversity. It is based on self/non-self pollen–pistil recognition interactions followed by inhibition of self-pollen hydration, germination, or pollen tube growth.

In the Brassicaceae, SI is sporophytically controlled by a multiallelic locus termed the *S* locus (Bateman, 1955). Male and female determinants have been identified as SP11/SCR (*S*-locus protein 11/*S*-locus cysteine-rich) (Schopfer *et al.*, 1999; Takayama *et al.*, 2000) and SRK (*S* receptor kinase)

(Takasaki *et al.*, 2000), respectively. When a compatible pollen grain lands on the stigma, it swells and a pollen tube is allowed to grow, whereas when self-pollen attaches to the stigma, SP11/SCR binds specifically to the extracellular domain of SRK of the same *S*-haplotype (Takayama *et al.*, 2001), which triggers an SI signalling pathway to reject self-pollen. Another stigmatically expressed gene located at the *S* locus, *S* locus glycoprotein (*SLG*) (Nasrallah *et al.*, 1987; Takayama *et al.*, 1987), has been shown to enhance the recognition process between self-pollen and stigma (Takasaki

Abbreviations: InDel, insertion/deletion; LG, linkage group; LOD, log of odds; QTL, quantitative trait locus; RFLP, restriction fragment length polymorphism; RLSICO₂, reaction level of SI to CO₂; SI, self-incompatibility; SSR, simple sequence repeat.

© The Author 2013. Published by Oxford University Press on behalf of the Society for Experimental Biology.

This is an Open Access article distributed under the terms of the Creative Commons Attribution License (<http://creativecommons.org/licenses/by/3.0/>), which permits unrestricted reuse, distribution, and reproduction in any medium, provided the original work is properly cited.

et al., 2000); however, this function of *SLG* remains controversial (Silva *et al.*, 2001). A recent study suggested that the plants in the Brassicaceae genus *Leavenworthia* use paralogous *SRK* and *SP11/SCR* genes, *Lal2* (*Leavenworthia alabamica SRK-related 2*) and *SCR1* (*SCR-like*), for self/non-self recognition in SI, but the function of their orthologues in other Brassicaceae genera also remains unknown (Chantha *et al.*, 2013).

Many studies focusing on the downstream components involved in this type of SI signalling pathway have been performed and, thus far, two components have been identified as positive effectors. ARC1 (arm repeat containing 1) was identified by a yeast two-hybrid screen using the kinase domain of SRK as the bait (Gu *et al.*, 1998; Stone *et al.*, 1999). ARC1 is a U-box protein with E3 ubiquitin ligase activity (Stone *et al.*, 2003), and has been shown to interact with Exo70A1, a putative component of the exocyst complex required for compatible pollination (Samuel *et al.*, 2009). MLPK (*M*-locus protein kinase) was identified by positional cloning as the gene responsible for the self-compatible mutation of *Brassica rapa* var. Yellow sarson (Murase *et al.*, 2004). MLPK is a membrane-anchored cytoplasmic protein kinase and interacts directly with SRK to transduce SI signalling (Kakita *et al.*, 2007). However, the importance of these two components in the Brassicaceae SI mechanism remains controversial (Kitashiba *et al.*, 2011; Indriolo *et al.*, 2012).

In the Brassicaceae, it has been known that SI can be overcome under some physiological and environmental conditions such as plant age (Ockendon, 1978; Horisaki and Niikura, 2008), stigmatic chemical treatments (e.g. ether, KOH, and NaCl) (Tatebe, 1968; Tao and Yong, 1986; Monterio and Gabelman, 1988), and high temperature (Matsubara, 1980; Okazaki and Hinata, 1987). CO₂ gas (3–5%) treatment (Nakanishi *et al.*, 1969) is the most effective way to overcome SI. Today, most cultivated lines of crucifer vegetables, such as cabbage, broccoli, Chinese cabbage, and radish are F₁ hybrids whose seeds are produced by mix-planting two self-incompatible inbred parental lines. In this economical F₁ hybrid breeding system, CO₂ gas treatment has been used to suppress SI and allow self-fertilization, thereby providing large-scale seed propagation of parental lines. This method has been used all over the world for many years, but the molecular mechanism leading to SI breakdown by CO₂ gas treatment is entirely unknown.

Previous studies suggested that not all lines respond equally to CO₂, and there are variations in SI response to CO₂ (CO₂ sensitivity) in the Brassicaceae (Nakanishi and Hinata, 1973; Niikura and Matsuura, 2000). Preliminary genetic analysis using lines with different CO₂ sensitivity in radish (*Raphanus sativus*) suggested that high CO₂ sensitivity was controlled by a recessive gene independent of the *S*-locus (Niikura and Matsuura, 2000). In another genetic analysis using CO₂-sensitive and CO₂-insensitive lines of Chinese cabbage (*B. rapa*), high CO₂ sensitivity was suggested to be controlled by a dominant gene (Hyun *et al.*, 2007); however, no responsible genes have been identified from these studies so far.

In this study, new inbred lines of *B. rapa* with different CO₂ sensitivity, a CO₂-sensitive line (HA-11621) and a CO₂-insensitive line (HA-11623), were selected and analysed.

X-ray microanalysis suggested that SI breakdown in the CO₂-sensitive line was accompanied by significant calcium accumulation at the pollen–stigma interface. Independent pre-treatment of pollen or pistil with CO₂ gas before pollination showed no effect on the SI reaction, suggesting that some physiological process that occurs after pollination is necessary for SI to be overcome. Genetic analyses using F₁ and F₂ progeny of a CO₂-sensitive × CO₂-insensitive cross suggested that CO₂ sensitivity is a semi-dominant and quantitative trait. Furthermore, quantitative trait locus (QTL) analyses identified two major responsible loci, *BrSIO1* and *BrSIO2*, which function additively in overcoming SI during CO₂ treatment.

Materials and methods

Plant materials

Two inbred lines of *B. rapa* ($2n=20$), a CO₂-sensitive line (HA-11621) and a CO₂-insensitive line (HA-11623), were established at Tohoku Seed Co., Ltd, and grown in the greenhouse with 16 h light and 8 h dark conditions at 20 °C. Both lines show stable SI under normal (open-air) condition but have different CO₂ sensitivity; SI in HA-11621 breaks down following treatment with 4.5% CO₂ whereas SI in HA-11623 is unaffected. HA-11621 and HA-11623 are reciprocally compatible, and their F₁ progeny were obtained under normal conditions. Buds (1–2 d before flowering) from a randomly chosen F₁ were used for F₂ production. Young petals and stamens were removed from the bud, and the immature pistil was pollinated with pollen grains from mature flowers of the same plant (bud pollination). Pollinated pistil was then covered with a paper bag for 3 d and seeds from the pistil were harvested. More than 20 pistils were pollinated, and harvested seeds were used as the F₂ population. A total of 110 F₂ plants were used for phenotypic and genetic analysis.

Cryo-scanning electron microscopy and energy-dispersive X-ray analysis

Flowers were self- or cross-pollinated and incubated for 1.5 h with or without 4.5% CO₂ gas. These pollinated and non-pollinated pistils were submerged in liquid nitrogen slush and frozen under vacuum. While under vacuum, the sample was transferred to the microscope cryo stage (ALTO 1000, Gatan), and then the stage temperature was increased to –95 °C to remove frost that had settled on top of the specimen as a result of condensation. When all surface frost had been removed by sublimation, as verified by electron microscopy, the temperature was reduced to –140 °C. Imaging was performed using an ETD (Everhart–Thornley detector) by Quant 250 scanning electron microscopy (FEI). The chamber pressure was 30 Pa and the accelerating voltage was 15 kV. EDX (energy-dispersive X-ray spectroscopy) analysis of the element assay was performed on selected papilla cells using INCA X-ray analysis software (Oxford Instruments, <http://www.oxinst.com/Pages/home.aspx>, last accessed 14 December 2013), with the detector's processing time set at 2. X-ray data were collected with 4.5 nA probe current for 2 min. Each 2–3 pistils were used in one experiment and three individual experimental sets were performed.

Evaluation of reaction level of SI to CO₂ (RLSICO₂)

Three to five flowers were cut at the peduncle and stood on a 1% (w/v) solid agar plate. Flowers were self-pollinated, placed into a CO₂ incubator, and treated with 4.5% CO₂ for 4 h at 23 °C. After 1 d at room temperature, pistils were fixed in ethanol:acetic acid (3:1) overnight, softened in 1 N NaOH at 60 °C for 2 h, then stained with 0.01% (w/v) decolorized aniline blue in 2% K₃PO₄ for 6 h. Pollen tube behaviour was observed under a fluorescent microscope (Axiophot 2, Zeiss). CO₂ sensitivity was measured using the RLSICO₂ index.

RLSICO₂ was classified into five categories, based on the number of pollen tubes penetrating into the stigma: 1, 0 pollen tubes; 2, 1–5 pollen tubes; 3, 6–15 pollen tubes; 4, 16–30 pollen tubes; and 5, >30 pollen tubes. Three replicates were performed on each plant on different days. Non-CO₂-treated self-pollinated flowers were used as controls. In all cases, no pollen tubes penetrated into the control stigmas.

Genotyping of S-haplotypes

S-haplotypes of *B. rapa* were identified using primers PS5 (5'-ATGAAAGGCGTAAGAAAAACCTA-3') and PS15 (5'-CCG TGTTTTATTTTAAGAGAAAGAGCT-3') (Nishio *et al.*, 1996) to amplify a fragment of the *SLG* gene. PCR-RFLP (restriction fragment length polymorphism) was used to distinguish the two S-haplotypes based on differential digest with the restriction enzyme *Kpn*I (TaKaRa, Japan). Digested DNA was electrophoresed on a 1.5% agarose gel.

Molecular markers and detection of DNA polymorphism

To screen for markers that show polymorphism between *B. rapa* lines, primers specific for simple sequence repeat (SSR) markers from different sources [UK, prefixes Ra, Na, Ol, and ENA (Lowe *et al.*, 2004; <http://brassica.bbsrc.ac.uk>); Japan, prefixes BRMS, KBr, and EST (Suwabe *et al.*, 2002, 2004, 2006; <http://vegmarks.nivot.affrc.go.jp>, NIVTS); China, prefix sau_um (Ge *et al.*, 2011); and Korea, prefix AMCP (Ramchiary *et al.*, 2011)] were used. SSR, RFLP, and insertion/deletion (InDel) markers (prefixes XT and Bra) were also designed based on the *Brassica* database (BRAD) (<http://brassicadb.org/brad/>, last accessed 14 December 2013) (Supplementary Table S1 available at *JXB* online).

Total genomic DNA was extracted from young leaves of two parental lines and F₂ progeny using the cetyltrimethylammonium bromide (CTAB) method (Murray and Thompson, 1980). DNA polymorphism analysis with SSRs was carried out using PCR with fluorescent dyes, performed according to Suwabe *et al.* (2008) with some modifications. The M13 (–21) universal primer sequence (18 bp) was fused to the 5' end of the original forward primer, and the M13 (–21) universal primer was labelled with 6-FAM, NED, VIC, or PET fluorescent dye (Applied Biosystems, CA, USA). PCRs were performed in a 10 µl reaction volume containing 10 ng of template DNA, 4.7 µM of labelled M13 (–21) universal primer and reverse primer, 0.3 µM of forward primer, 1× PCR buffer, 1× dNTP, 1× MgCl₂, and 0.5 U of rTaq (TOYOBO, Japan). Conditions for PCR were as follows: initial denaturation was carried out at 94 °C for 3 min followed by 37 cycles at 94 °C for 30 s, 55 °C (slope of 0.5 °C s^{–1}) for 30 s, 72 °C (slope of 0.5 °C s^{–1}) for 30 s, and a final extension at 72 °C for 4 min. A 1 µl aliquot of 50-fold diluted PCR product was added to 8.9 µl of Hi-Di™ Formamide and 0.1 µl of GeneScan™ 600 LIZ™ Size Standard (Applied Biosystems, USA) and applied to an ABI 3730 DNA Analyzer (Applied Biosystems). Data were analysed using ABI GeneMapper® software.

For polymorphism analysis with RFLP and InDel markers, PCR was carried out in a 10 µl reaction volume with 5 pmol of forward and reverse primers instead of fluorescent dyes. For RFLP markers, amplified fragments were digested using restriction enzymes for 1 h. Fragments of digested DNA were separated on a 2–4% agarose gel.

Linkage map construction and QTL analysis

A genetic map was constructed using JoinMap® version 4 (Van Ooijen, 2006) utilizing the double pseudo-testcross strategy with a log₁₀ of odds (LOD) threshold of 6.0 for linkage group identification. The best marker order was calculated with the regression mapping algorithm, and marker order was retained from the first round only. Map distance units in centiMorgans (cM) were converted from recombination frequencies using the Kosambi mapping function (Kosambi, 1944). Interval mapping (IM) was performed to identify putative QTLs using the established linkage map and the observed

phenotypic traits. This method was run using MapQTL® version 6 (Van Ooijen, 2009). With this software, a *P* < 0.05 LOD score significance threshold was calculated by creating a group-wide distribution of the data based on a 1000 permutation test. LOD peaks were used to estimate the position of QTLs on the map.

Statistical analysis

Box plots were prepared by Ekuseru-Toukei 2012 software (Social Survey Research Information Co., Ltd, Japan) to compare the phenotypic difference, as this plot type gives a good sense of environmental data distribution (Upton and Cook, 1996). Kruskal–Wallis analysis of variance (ANOVA) by ranks was used between paired comparisons of markers to examine marker association.

Results

Phenotypic analysis of *B. rapa* lines in response to CO₂ treatment

Two inbred lines of *B. rapa* with different CO₂ sensitivity, a CO₂-sensitive line (HA-11621) and a CO₂-insensitive line (HA-11623), were used in this study. Flowers were self-pollinated by hand pollination and incubated in a CO₂ incubator (4.5% CO₂) for 4 h. Both lines were self-incompatible under normal conditions (control) (Fig. 1A, B), whereas they showed significantly different responses to CO₂ gas treatment (Fig. 1C, D). Specifically, in the CO₂-sensitive line, many pollen tubes were seen to penetrate into papilla cells after CO₂ treatment. This pollination test confirmed that the CO₂-sensitive line had high sensitivity to CO₂ while the CO₂-insensitive line hardly responded to 4.5% CO₂. Cross-pollination was performed as a positive control (Fig. 1E, F).

Physiological changes in papilla cells after CO₂ treatment

Previous work using X-ray microanalysis has revealed the accumulation of calcium at the stigmatic surface following compatible cross-pollination in *Brassica oleracea* (Elleman and Dickinson, 1999). X-ray mapping strongly indicated that a high concentration of calcium was localized at the points where the pollen grain made contact with the surface of the stigmatic papilla cell. The calcium accumulation was also observed in *B. rapa*, especially in compatible pollination (Iwano *et al.*, 1999). To examine the physiological effect of CO₂ on pollination reactions, this calcium accumulation was examined by using cryo-scanning electron microscopy fitted with an X-ray microanalysis system. When the CO₂-sensitive line was cross-pollinated with the CO₂-insensitive line, pollen grain hydrated and the pollen tube penetrated into the papilla cell, but when CO₂-sensitive and CO₂-insensitive lines were self-pollinated under normal conditions (without CO₂ treatment), few pollen grains hydrated, and no pollen tube germination was observed in either line (Fig. 2A, upper panel). After CO₂ treatment, the cross-pollinated pollen grains did not show a significant difference, neither did the self-pollinated CO₂-insensitive line. However, the self-pollinated CO₂-sensitive line showed obvious changes: pollen hydration and germination were observed under CO₂ treatment (Fig. 2A,

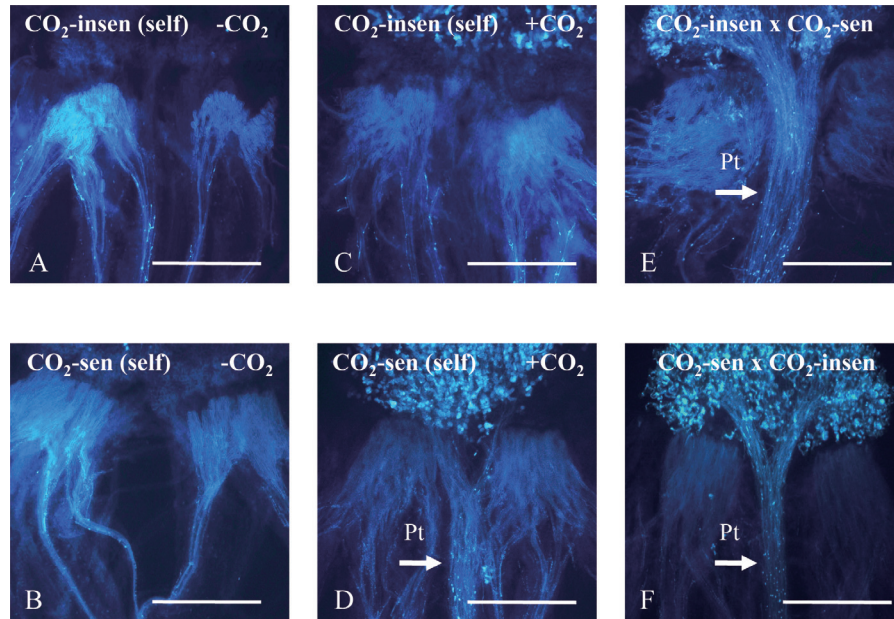


Fig. 1. Phenotype of inbred *Brassica rapa* lines used in this study. (A, B) Pollen tube behaviour after self-pollination of CO₂-sensitive (HA-11621) and CO₂-insensitive (HA-11623) lines under normal conditions (without CO₂ treatment). No penetrated or elongated pollen tubes are observed in either line. (C, D) Pollen tube behaviour after self-pollination of CO₂-sensitive and CO₂-insensitive lines under 4.5% CO₂ gas treatment. Pollen tubes could penetrate into the stigma and elongate through the style only in the CO₂-sensitive line. (E, F) Cross-pollination as a positive control; the arrow shows pollen tubes which have penetrated. Pt, pollen tubes. Bar=1000 μm.

lower panel). The emission of elements (K α) in the tip of the papilla cells was then analysed after selecting the pollinated papilla cells which faced nearly the same direction in relation to the X-ray detector. Emissions of P-K α , S-K α , K-K α , and Ca-K α were detected together with C and O, which are constituent elements of biological materials. The detected emission of Al-K α originates from the stub that held the samples (Fig. 2B). There was no significant difference in the elemental emissions between CO₂-sensitive and CO₂-insensitive lines before pollination. Ca²⁺ accumulation was observed after cross-pollination as previously reported (Iwano et al., 1999), and Ca-K α emission was increased with CO₂ treatment. After self-pollination, Ca-K α emission was slightly increased in the CO₂-sensitive line in the normal CO₂ condition. This Ca-K α increase became more pronounced (~6-fold) in the CO₂-sensitive line when it was self-pollinated in the high CO₂ condition. In the CO₂-insensitive line, no significant Ca-K α increase was observed after self-pollination in normal or high CO₂ conditions (Fig. 2B). Although the biological significance of the accumulation of calcium at the pollen–stigma interface is not clear, it has been suggested that calcium plays some role in the successful development of the pollen tube tip into the region of expanded stigmatic wall (Elleman and Dickinson, 1999). The present results suggest that, in the CO₂-sensitive line, high CO₂ activates a compatible pollination pathway or disturbs an SI signalling pathway leading to Ca²⁺ accumulation at the pollen–stigma interface.

The efficiency of CO₂ treatment

A previous study suggested that the effect of CO₂ on SI breakdown depends on the timing of treatment (Nakanishi

and Hinata, 1973). In the CO₂-sensitive line, when self-pollinated flowers were immediately treated with 4.5% CO₂ for 4 h, SI could be overcome, and typically >10 pollen tubes penetrated into the stigma (Fig. 3A). When CO₂ treatment started 3 h after self-pollination, SI could still be overcome (Fig. 3B). However, when CO₂ treatment started 6 h after self-pollination, the number of penetrating pollen tubes was decreased (Fig. 3C). These results indicate that self-pollen inhibition in SI is biostatic, as previously suggested (Sarker et al., 1988), and can be reversed at least at 3 h after pollination. However, at 6 h after pollination, SI inhibition enters an irreversible phase that cannot be overcome by CO₂ treatment.

Next, in order to narrow down the stage of SI affected by CO₂ treatment, experiments with high CO₂-pre-treated pollen or pistil from the CO₂-sensitive line were performed (Fig. 4). SI could not be overcome by pre-treatment of either tissue, and no pollen tube penetration could be observed even when both pollen and pistil were treated separately prior to pollination (Fig. 4). SI could be overcome only when the self-pollinated pistil was treated with high CO₂. These results suggest that some post-pollination physiological process is affected by high CO₂, in the process of SI breakdown.

S-allele characterization and phenotype of CO₂ sensitivity in F₁ and F₂

The S-haplotypes of the two parental inbred lines were first determined by amplifying their SLG genes (Nishio et al., 1996). The sequence data suggested that the S-haplotypes of the CO₂-sensitive and CO₂-insensitive lines were S₅₅S₅₅ and S₄₆S₄₆, respectively. To dissect genetically the gene(s) that determines sensitivity to CO₂ treatment, six F₁ plants

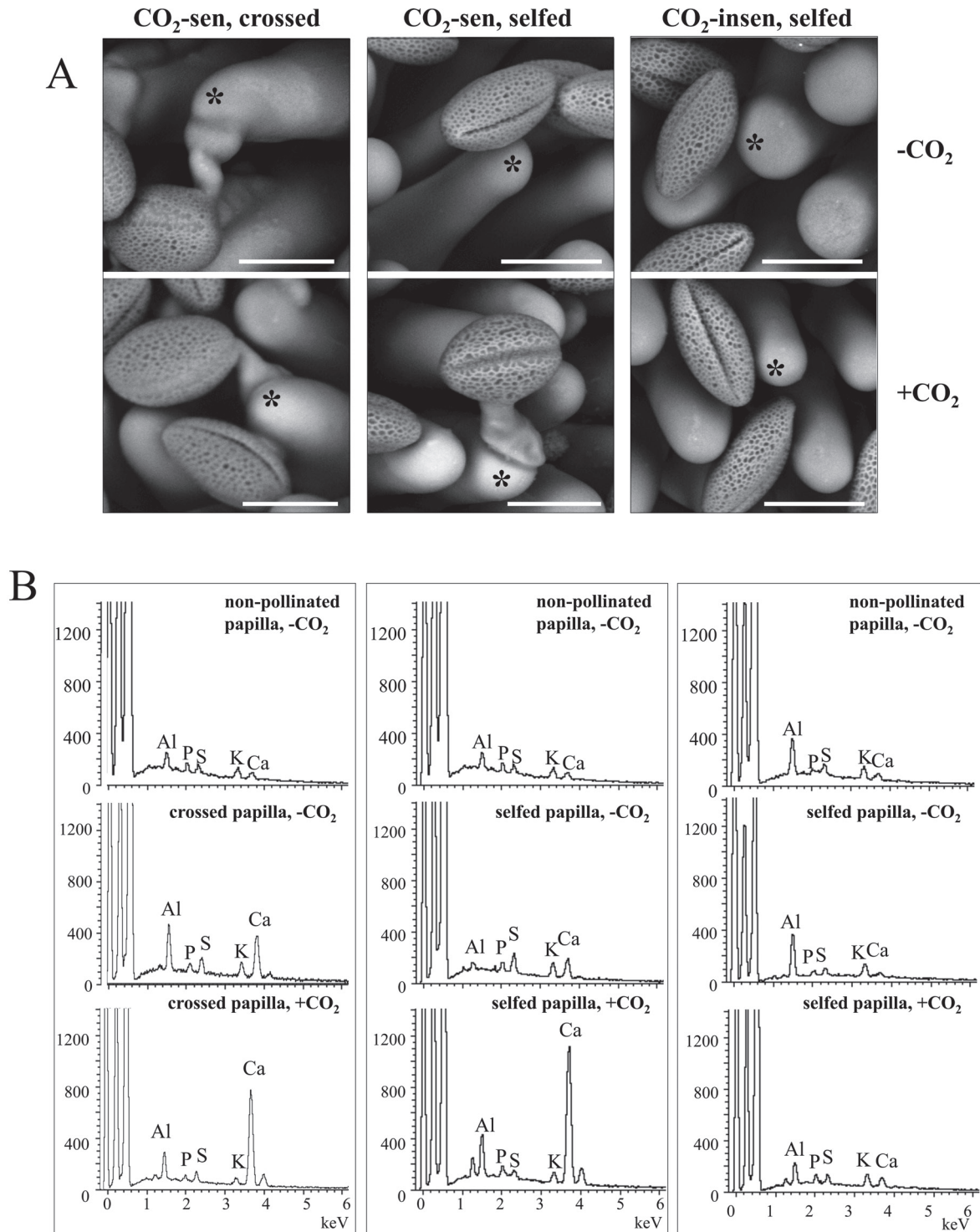


Fig. 2. Electron micrographs and X-ray microanalysis of *B. rapa*. (A) Cryo-scanning electron micrographs of pollinated papilla cells were taken 1.5 h after pollination. Representative examples of the cross-pollinated (left column) and self-pollinated (middle column) CO₂-sensitive line, and the self-pollinated (right column) CO₂-insensitive line are shown. Without CO₂ treatment (upper panels), only cross-pollen is accepted, and self-pollen grains maintain a spheroid shape without swelling in both lines. With 4.5% CO₂ gas treatment (lower panels), pollen grains swell and germinate in the CO₂-sensitive line (lower middle) but not in the CO₂-insensitive line (lower right). Bar=25 μm. (B) Representative examples of energy-dispersive X-ray spectra of non-pollinated and pollinated papilla cell surfaces. Scanning positions for X-ray analyses are indicated by asterisks in (A). The emissions of Al-Kα, P-Kα, S-Kα, K-Kα, and Ca-Kα were detected at the papilla cell surfaces, and the intensity of Ca emission was increased after cross-pollination (left column). The increase of Ca emission was also observed after self-pollination with 4.5% CO₂ gas treatment in the CO₂-sensitive line (middle column) but not in the CO₂-insensitive line (right column). These spectrum patterns are reproducible in three individual experiment sets. The emission of Al-Kα is mostly derived from the stub that held the samples.

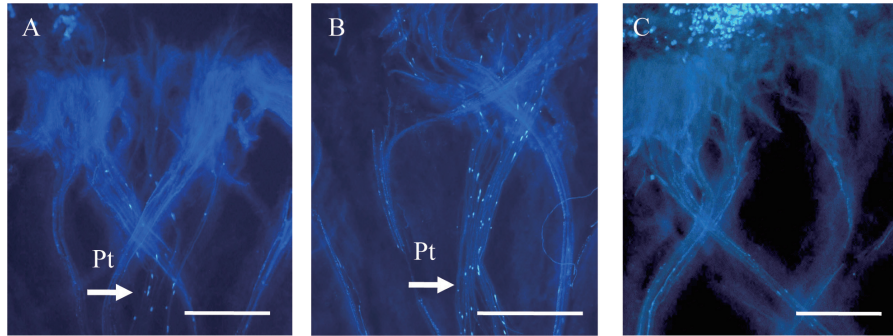


Fig. 3. The efficiency of CO₂ treatment of the CO₂-sensitive line. (A) Self-pollinated stigmas were treated with 4.5% CO₂ immediately after self-pollination, and pollen tube penetration and elongation were observed. (B) Self-pollinated stigmas were treated with 4.5% CO₂ 3h after self-pollination. The pollen tube can still penetrate into papilla cells. (C) When CO₂ treatment began 6h after self-pollination, the number of penetrating pollen tubes was decreased. Pt, pollen tubes. Bar=1000 μm.

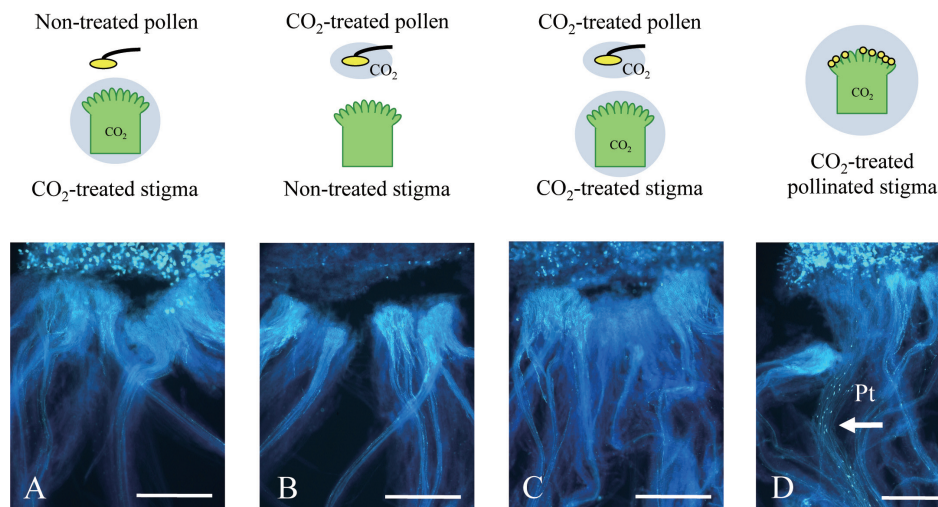


Fig. 4. Pollination assay using CO₂-treated non-pollinated flowers of the CO₂-sensitive line as either CO₂-treated pistil or pollen. Pollen tube behaviour is observed after a 4h CO₂ treatment immediately after self-pollination. (A) A pistil from a non-pollinated flower treated with CO₂ for 4h was pollinated with pollen from the same plant which was not treated with CO₂. (B) A pistil from a non-treated non-pollinated flower was pollinated with pollen from the same plant which was treated with CO₂ for 4h. (C) A pistil from a CO₂-treated non-pollinated flower (CO₂-treated) was pollinated with pollen from the same plant which was treated with CO₂ for 4h. (D) Self-pollinated flower treated with CO₂ after pollination, positive control. Pt, pollen tubes. Bar=1000 μm.

(*S*_{46*S*₅₅) were produced by crossing CO₂-sensitive and CO₂-insensitive lines. These F₁ plants exhibited an intermediate CO₂ sensitivity phenotype where self-pollen tubes penetrated into the stigma under high CO₂ treatment but there were fewer penetrating pollen tubes than observed in a self-pollination of the CO₂-sensitive parent. An F₂ population of 110 individuals derived from a bud-pollinated F₁ plant was made and used for further genetic analyses of the CO₂ sensitivity. F₂ individuals were genotyped using PCR-RFLP to distinguish *SLG* alleles (Supplementary Fig. S1 at JXB online). *S*₅₅- and *S*₄₆-haplotypes were segregated in the F₂ population according to Mendelian transmission (Supplementary Table S2). Pollen tube behaviour after CO₂ treatment varied among individuals and, in order to quantify the strength of CO₂ sensitivity, the modified RLSICO₂ (reaction level of SI to CO₂) index was employed (Niikura and Matsuura, 2000), which calculates CO₂ sensitivity based on the number of penetrating pollen tubes after self-pollination under high CO₂}

conditions (see the Materials and methods). The RLSICO₂ of 110 F₂ individuals is presented in Supplementary Fig. S2, and the summarized box-plot data are shown in Fig. 5, together with the RLSICO₂ of F₁ and the parental inbred lines. F₁ had an RLSICO₂ score intermediate to the two parental lines, suggesting that the high CO₂ sensitivity is a semi-dominant (incompletely dominant) trait in these inbred lines. Furthermore, the RLSICO₂ of F₂ individuals was continuously distributed and did not follow a simple one-locus biallelic Mendelian distribution (Supplementary Fig. S2). These results suggest that CO₂ sensitivity in the inbred lines used here could be a quantitative trait which is controlled by more than one gene.

Relationship between *S*-alleles and CO₂ sensitivity

To investigate whether CO₂ sensitivity is related to *S*-haplotypes, the 110 F₂ individuals were grouped into three

genotypes ($S_{55}S_{55}$, $S_{46}S_{46}$, and $S_{46}S_{55}$). The RLSICO₂ of each group is shown in Fig. 5. In the three F₂ groups, RLSICO₂ scores were distributed from 1 to 5, and interquartile ranges overlapped, indicating that CO₂ sensitivity is not linked to the *S*-locus in these two lines.

Reproductive tissue controlling CO₂ sensitivity

From the F₂ population, two $S_{46}S_{46}$ homozygotes with different RLSICO₂ were selected: F₂-16, a CO₂-insensitive line (RLSICO₂=1±0); and F₂-26, a CO₂-sensitive line (RLSICO₂=4.15±0.53). These two lines were used to examine the reproductive tissue controlling CO₂ sensitivity. Reciprocal crosses were performed between these two SI lines with or without high CO₂ gas treatment. Because all crosses under normal conditions (without CO₂ treatment) were incompatible, only data from crosses performed in the high CO₂ condition are shown in Fig. 6. The cross between

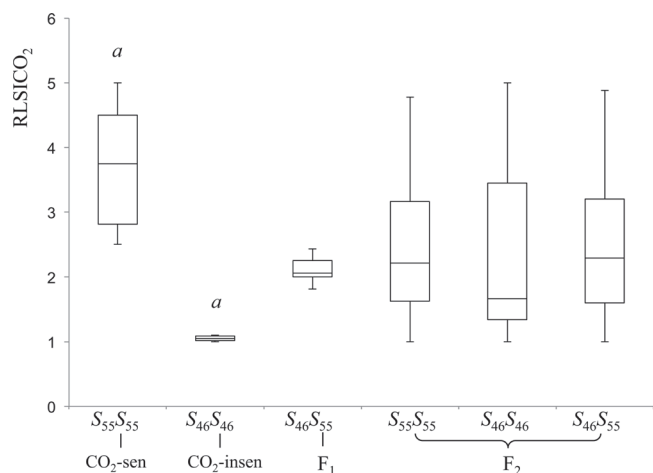


Fig. 5. Box plots of CO₂ sensitivity phenotypes. Data show the distribution of RLSICO₂ with 25th, 50th, and 75th percentiles (horizontal bars), interquartile ranges (columns), and 1.5 interquartile ranges (error bars) of RLSICO₂ from six CO₂-sensitive ($S_{55}S_{55}$) and six CO₂-insensitive ($S_{46}S_{46}$), individuals, six F₁ individuals ($S_{46}S_{55}$), and 110 F₂ individuals (22 $S_{46}S_{46}$, 64 $S_{46}S_{55}$, and 24 $S_{55}S_{55}$). *a* indicates a significant difference ($P < 0.01$) between CO₂-sensitive and CO₂-insensitive lines.

CO₂-sensitive F₂-26 pistil and CO₂-insensitive F₂-16 pollen was CO₂ sensitive, showing many penetrating pollen tubes under high CO₂. On the other hand, the cross between CO₂-insensitive F₂-16 pistil and CO₂-sensitive F₂-26 pollen was CO₂ insensitive, showing no penetrating pollen tubes even under high CO₂. These results suggest that CO₂ sensitivity is controlled by genes expressed in the female tissue (pistil).

Marker analysis and construction of a linkage map

In order to map QTLs that determine CO₂ sensitivity, a linkage map was constructed for this F₂ population. A total of 911 different genetic markers were examined in the two parental lines. To clarify the relationship between previously identified SI-related genes and CO₂ sensitivity, *SLG* (an *S*-locus marker), *MLPK*, and *ARCI* were also selected. Though a very low level of polymorphism (14.7%) was detected for all types of markers, 123 polymorphic markers were selected, which include 113 SSRs, five RFLPs, and five InDel markers. These 123 markers were used for linkage mapping, and generated 10 linkage groups (A01–A10) at a LOD threshold value of 6.0 (Fig. 7). The total length of the map was 947.5 cM, and the length of the linkage groups ranged from 63.2 cM (A10) to 168.4 cM (A03). The distance between markers varied from 0 to 29.3 cM, with an average interval of 7.7 cM. *SLG*, *MLPK*, and *ARCI* were mapped to A07, A03, and A04, respectively, which is consistent with previous reports (Ajisaka *et al.*, 2001; Hatakeyama *et al.*, 2010).

QTL analysis and association of markers with high CO₂ sensitivity

Using the constructed linkage map, QTLs responsible for high CO₂ sensitivity were analysed. Three QTLs were identified on linkage groups A03 and A05 based on a LOD threshold of 3.40 (1000 permutation test, $P < 0.05$) (Fig. 8, Table 1). These QTLs were tentatively named *Brassica rapa SI Overcome (BrSIO) 1–3*, and these results further supported the prediction that CO₂ sensitivity of SI is controlled by a polygenic system. *BrSIO1* on A05 and *BrSIO2* on A03 are two major QTLs that explained 19.3% and 19.0% of phenotypic variation, respectively. *BrSIO3*, located near *BrSIO2*, accounted for 14.5% of the variance (Table 1).

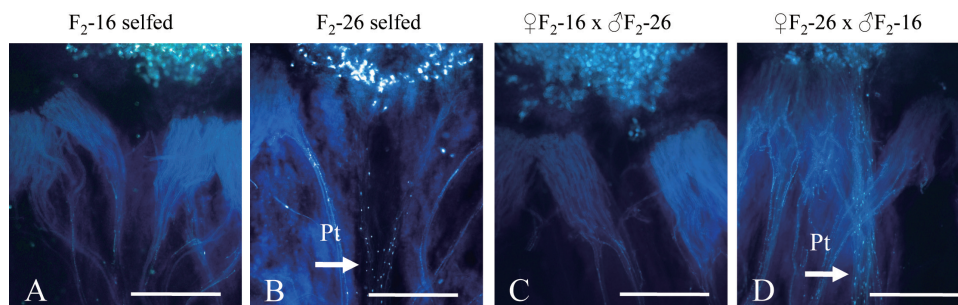


Fig. 6. Reciprocal crosses with CO₂ treatment between two S_{46} homozygous individuals from the F₂ population with different RLSICO₂. (A) CO₂-sensitive F₂ self-pollination. (B) CO₂-insensitive F₂ self-pollination. (C) A CO₂-sensitive F₂ pistil pollinated with pollen from a CO₂-insensitive F₂. (D) A CO₂-insensitive F₂ pistil pollinated with pollen from a CO₂-sensitive F₂. Pt, pollen tubes. Bar=1000 μm. $n=3$.

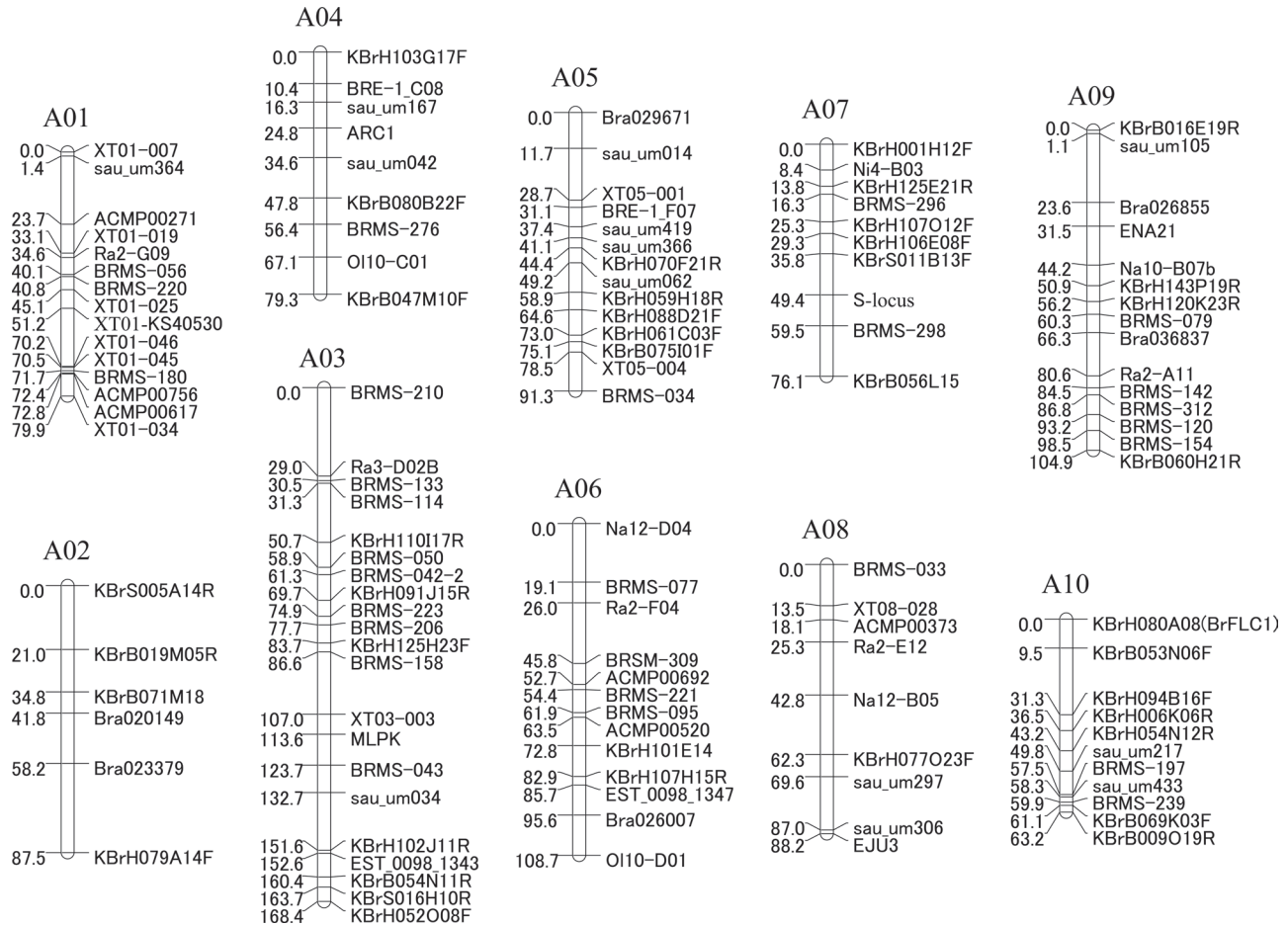


Fig. 7. A linkage map of selected DNA markers from the F_2 population. Map distances are shown to the left of vertical lines of the linkage group in cM, and marker names are shown to the right.

To examine the significance of these QTLs, F_2 progeny were classified into groups based on the genotypes of the linkage markers nearest these three newly identified loci, and the relationship of the loci to RLSICO₂ in individual plants was analysed using Kruskal–Wallis ANOVA by ranks (Table 2). Alleles from CO₂-sensitive (HA-11621) and CO₂-insensitive (HA-11623) lines are presented as *S* and *I*, respectively. Almost all classifications using the closest linkage markers showed a higher RLSICO₂ index in the *SS* group with significance at $P < 0.01$, except marker BRMS-114, which showed significance at $P < 0.05$.

Marker association was further examined with combinations of *BrSIO1* and *BrSIO2* since *BrSIO3* is a minor QTL closely linked to *BrSIO2*, making it difficult to identify it as an independent QTL. F_2 progeny were classified into nine groups based on the genotypes of their closest linkage markers (Table 3). According to this classification, for example, the two above analysed $S_{46}S_{46}$ homozygous lines with different RLSICO₂, F_2 -16 (CO₂-insensitive line) and F_2 -26 (CO₂-sensitive line), were classified into group 8 and group 1, respectively. When groups with the same *BrSIO1* genotype were compared, the *BrSIO2 SS* group showed a higher RLSICO₂ index compared with the *BrSIO2 II* group. Likewise, when the groups with the same *BrSIO2* genotype were compared, the *BrSIO1 SS* group showed a higher

RLSICO₂ compared with the *BrSIO1 II* group. Although the numbers of F_2 individuals in each group were rather low, significance ($P < 0.05$) was detected between groups 1 and 6, 2 and 6, and 2 and 8. These data suggest that *BrSIO1* and *BrSIO2* work additively in overcoming SI during CO₂ treatment in the CO₂-sensitive (HA-11621) line. No QTL was detected at genes known to affect SI stability (*MLPK*, *ARC1*, or the *S*-locus), indicating that CO₂ sensitivity is determined by novel genes in the experimental lines used here.

Associated gene prediction by in silico comparative mapping

Using the *B. rapa* genome sequence (Cheng et al., 2011), *BrSIO1* could be mapped to a 569 kb region flanked by InDel marker XT05-004 and SSR marker BRMS-034, and *BrSIO2* to a 1469 kb region flanked by SSR markers BRMS-042-2 and KBrH110I17R. These two regions include 121 and 280 genes annotated in the *Brassica* database (BRAD), respectively (Supplementary Tables S3, S4 at JXB online). Comparison of the *A. thaliana* genome with the Brassicaceae genome (reviewed by Schranz et al., 2006) suggests that *BrSIO1* has synteny on *A. thaliana* chromosome 2 and *BrSIO2* has synteny on both chromosomes 3 and 4. It is assumed that these two QTLs do not have the same genetic origin and could be

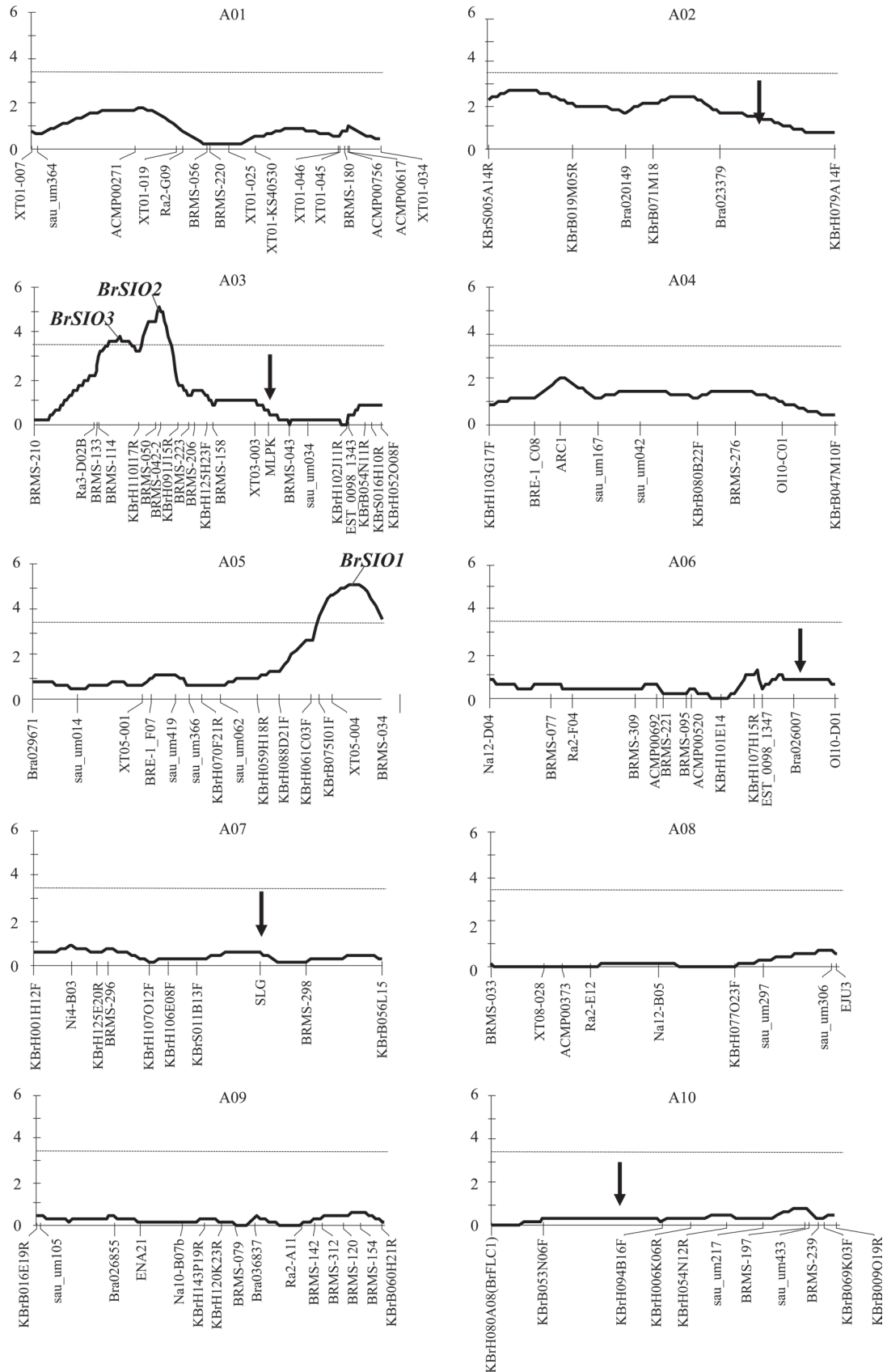


Fig. 8. QTL analysis results. The solid line indicates the LOD score and the dotted line indicates the QTL threshold (LOD=3.4) determined using a 1000 permutation test ($P < 0.05$). The x-axis represents each linkage group (cM) and the y-axis indicates the QTL score. Two QTLs (*BrSIO2* and 3) are detected in A03 and one in A05 (*BrSIO1*). Arrows show loci involved in SI stability reported by Hatakeyama *et al.* (2010).

Table 1. Summary of CO₂ sensitivity QTLs

QTL	LG	Closest marker	QTL peak (cM) ^a	LOD	R ^{2b}	Additive effect ^c
<i>BrSIO1</i>	A05	XT05-004	83.50	5.17	19.30	0.72
<i>BrSIO2</i>	A03	BRMS-042-2	60.87	4.46	19.00	0.69
<i>BrSIO3</i>	A03	KBrH110117R	41.25	3.76	14.50	0.65

^a QTL peak position, detected by interval mapping, between two markers.

^b Amount of phenotypic variation explained by the QTL.

^c Additive effect of the CO₂-sensitive HA-11621 allele on RLSICO₂.

Table 2. Statistical analysis of QTL effect

QTL	<i>BrSIO1</i>		<i>BrSIO2</i>		<i>BrSIO3</i>		
Marker ^a	KBr B075I01F	XT05-004	BRMS-034	BRMS-042-2	BRMS-050	KBr H110117R	BRMS-114
SS	3.12 (27) ^b	3.17 (24) ^b	3.24 (20)	3.10 (23) ^b	3.09 (22)	3.01 (25)	3.01 (30)
SI	2.34 (53) ^{**}	2.36 (51) ^{**}	2.42 (52) ^{**}	2.43 (60) ^{**}	2.47 (63) ^{**}	2.45 (62) ^{**}	2.30 (54)
II	2.02 (26) ^{cd}	1.93 (25)	2.06 (33)	1.87 (23)	1.84 (22)	1.86 (22)	2.03 (22)

^a S, CO₂-sensitive HA-11621 allele; I, CO₂-insensitive HA-11623 allele.

^b Individuals whose genotype was unidentified are excluded.

^c Kruskal–Wallis analysis comparing phenotype between genotype groups with individuals in the same groups.

^d Significance level: ***P* < 0.01; **P* < 0.05.

Table 3. QTL association for CO₂ sensitivity

Group no.	Marker ^a		No. of individuals ^b	Mean RLSICO ₂
	XT05-004	BRMS-042-2		
1	SS	SS	5	3.86
2	SS	SI	13	3.23
3	SS	II	5	2.40
4	SI	SS	13	3.12
5	SI	SI	23	2.37
6	SI	II	13	1.63
7	II	SS	6	2.42
8	II	SI	16	1.78
9	II	II	3	1.71

^a S, CO₂-sensitive HA-11621 allele; I, CO₂-insensitive HA-11623 allele.

^b Individuals whose genotype was unidentified are excluded.

^c Significance level, **P* < 0.05.

two independent regions controlling high CO₂ sensitivity. Based on reciprocal cross results, the CO₂ sensitivity trait may be controlled by genes expressed in the female organ (Fig. 8). A total of 121 and 280 annotated genes in *BrSIO1* and *BrSIO2* have 103 and 243 homologues in *A. thaliana*, respectively, and 54 and 141 of these genes are expressed in *A. thaliana* pistil (microarray data of carpel at stage 12, http://affymetrix.arabidopsis.info/narrays/search.pl?fl=1&s1=ATGE_37, last accessed 14 December 2013, Supplementary Tables S3, S4).

Genes involved in related biological processes are often expressed cooperatively and their co-expression information is important for understanding biological systems (Eisen et al., 1998). ATTED-II (<http://atted.jp/>, last accessed 14 December 2013) is a gene co-expression database useful for identifying the potential partners working in the same biological processes (Obayashi et al., 2007). Co-expression analysis

was performed using ATTED-II with these 195 genes and it was found that *MAP kinase 6* (At2g43790 in *BrSIO1*) and *ethylene overproducer 1* (At3g511770 in *BrSIO2*) showed the strongest co-expression and *calmodulin-like 41* (At3g50770 in *BrSIO2*) has weak co-expression with *cytochrome c oxidase 10* (At2g44520 in *BrSIO1*) and *beta glucosidase 28* (At2g44460 in *BrSIO1*). In addition to these co-expressed genes, these two regions encode highly homologous family member proteins, for example matrixin proteins (At2g45040 in *BrSIO1* and At4g16640 in *BrSIO2*) and senescence-associated proteins (At2g44670 in *BrSIO1* and At4g17670 in *BrSIO2*). All these can be candidate responsible genes, although the biological functions of these genes are mostly unknown.

Discussion

It has been >40 years since Nakanishi et al. (1969) first reported that SI could be overcome by CO₂ and Nakanishi and Hinata (1973) demonstrated the applicability of this technique to commercial use. Nowadays, seed companies have adopted this method to obtain inbred parental seeds of crucifer vegetables for large-scale commercial F₁ hybrid seed production. However, there is still very limited understanding of the mechanism by which SI is overcome.

Lee et al. (2001) showed a shrunken and distorted papilla cell surface in the CO₂-sensitive *B. rapa* cv. Hiratsuka, and suggested that these structural changes could cause SI to be overcome. The cryo-scanning electron microscopy data reported here did not show any structural changes in CO₂-sensitive or CO₂-insensitive lines (Fig. 2A). Additionally, pre-treatment of non-pollinated pistils with high CO₂ gas did not cause SI breakdown (Fig. 4). Therefore, a completely different SI breakdown mechanism must be present, at least in

the CO₂-sensitive line. In contrast, massive Ca accumulation was observed at the pollen–stigma interface specifically in CO₂-sensitive plants under high CO₂ conditions (Fig. 2B). Brewbaker and Kwack (1963) were the first to describe the need for a high concentration of Ca²⁺ for pollen germination and pollen tube growth. The high concentration of Ca²⁺ could be needed for activating pectinase to loosen the papilla cell wall, allowing the pollen tube to penetrate (Black and Charlwood, 1995), or for keeping the pollen tube cell wall rigid enough not to burst (Hepler and Winship, 2010). Although causal relationships remain unclear, the data suggest that CO₂ treatment induces a certain compatible reaction leading to Ca²⁺ accumulation at the pollen–stigma interface.

To date, several genetic studies have been performed to understand the mechanism of SI breakdown for breeding purposes. Niikura and Matsuura (2002) reported that in Japanese radish high CO₂ sensitivity is controlled by a recessive gene that governs the construction and/or metabolism of the stigma, which reacts to CO₂ without any changes in gene expression. In contrast, Hyun *et al.* (2007) reported a dominant, *S*-haplotype-linked high CO₂ sensitivity phenotype in *B. rapa*. In contrast to these previous reports, F₁ plants had an intermediate CO₂ sensitivity and the F₂ population had a continuous frequency distribution of RLSICO₂ in the present study (Fig. 6). These results suggest that in the lines used for this study, CO₂ sensitivity is a quantitative trait which is controlled by more than one gene.

Genetic linkage maps based upon frequency of recombination in segregating populations are fundamental and powerful tools for associating phenotypic trait-specific genetic regions. Linkage mapping can be used to understand the biological basis of complex traits and to dissect genetic determinants underlying the expression of agronomically important breeding traits (Paran and Zamir, 2003). Using QTL analysis, two major QTLs for high CO₂ sensitivity were successfully identified (Fig. 8). *BrSIO1* and *BrSIO2* had similar LOD scores and explained similar amounts of phenotypic variation (19.3% and 19%), and these could be two major factors controlling high CO₂ sensitivity. Very recently, five QTLs associated with stability of SI in *B. rapa* have been identified. Two of them co-localized with *SLG* (A07) and *MLPK* (A03) and the other three were on A02, A06, and A10 (Hatakeyama *et al.*, 2010). CO₂ sensitivity did not link with the *S*-locus in the present study (Fig. 5) and none of the other reported loci co-localized with QTLs detected here (Fig. 8), indicating that CO₂ sensitivity of the lines in this study is determined by novel genes different from those known to affect SI stability. Genes in *BrSIO1* and *BrSIO2* regions have 103 and 243 homologues in *A. thaliana*, respectively, and 54 and 141 of these genes are expressed in *A. thaliana* pistil. *In silico* comparative analyses identified several co-expressing genes and highly homologous genes encoded in these two regions. All these can be candidate responsible genes; however, to identify the genes responsible for high CO₂ sensitivity in the QTL regions in *B. rapa* more accurately, it would be necessary to narrow down the regions by developing near-isogenic lines (NILs).

To maintain F₁ seed quality, inbred lines with strong but CO₂-sensitive SI are ideal for F₁ hybrid breeding, and it is very important to understand the genetic relationships between SI-related genes and CO₂ sensitivity phenotypes. These results could be useful for the marker-assisted selection of parental lines with both stable SI and high CO₂ sensitivity.

Supplementary data

Supplementary data are available at *JXB* online.

Figure S1. *S*-haplotype analysis of F₂ plants by PCR-RFLP.

Figure S2. RLSICO₂ in CO₂-sensitive and CO₂-insensitive lines, and F₁ and F₂ progeny based on the number of penetrating pollen tubes after self-pollination under high CO₂ conditions.

Table S1. Genetic markers and their primers used for linkage analysis.

Table S2. *S*-haplotype segregation in the F₂ population.

Table S3. Annotated genes and *Arabidopsis* homologues in *BrSIO1*.

Table S4. Annotated genes and *Arabidopsis* homologues in *BrSIO2*.

Acknowledgements

The authors thank Ms Rina Nagai, Ms Hitomi Ishikawa, and Ms Yuko Yoshimura for their excellent technical assistance. This work was supported by a Grant-in-Aid for the Scientific Research on Innovative Areas (21112003, 23113002) and by Grants in Aid for Scientific Research (23570056, 21248014, 25252021) from the Ministry of Education, Culture, Sports, Science and Technology of Japan (MEXT) and by the Japan Advanced Plant Science Network.

References

- Ajisaka H, Kuginuki Y, Yui S, Enomoto S, Hirai M. 2001. Identification and mapping of a quantitative trait locus controlling extreme late bolting in Chinese cabbage (*Brassica rapa* L. ssp. *pekinensis* syn. *campestris* L.) using bulked segregant analysis: a QTL controlling extreme late bolting in Chinese cabbage. *Euphytica* **118**, 75–81.
- Bateman AJ. 1955. Self-incompatibility systems in angiosperms. III. Cruciferae. *Heredity* **9**, 52–68.
- Black M, Charlwood B. 1995. *The physiology and biochemistry of plant cell walls*. London: Chapman & Hall.
- Brewbaker JL, Kwack BH. 1963. The essential role of calcium ion in pollen germination and pollen tube growth. *American Journal of Botany* **50**, 859–865.
- Chantha S-C, Herman AC, Platts AE, Vekemans X, Shoen DJ. 2013. Secondary evolution of a self-incompatibility locus in the Brassicaceae genus *Leavenworthia*. *PLoS Biology* **11**, e1001560.
- Cheng F, Liu S, Wu J, Fang L, Sun S, Liu B, Li P, Hua W, Wang X. 2011. BRAD, the genetics and genomics database for *Brassica* plants. *BMC Plant Biology* **11**, 136.

- Eisen MB, Spellman PT, Brown PO, Botstein D.** 1998. Cluster analysis and display of genome-wide expression patterns. *Proceedings of the National Academy of Sciences, USA* **95**, 14863–14868.
- Elleman CJ, Dickinson HG.** 1999. Commonalities between pollen/stigma and host/pathogen interactions: calcium accumulation during stigmatic penetration by *Brassica oleracea* pollen tubes. *Sexual Plant Reproduction* **12**, 194–202.
- Ge Y, Ramchiary N, Wang T, Liang C, Wang N, Wang Z, Choi SR, Lim YP, Piao ZY.** 2011. Development and linkage mapping of unigene-derived microsatellite markers in *Brassica rapa* L. *Breeding Science* **61**, 160–167.
- Gu T, Mazzurco M, Sulaman W, Matias DD, Goring DR.** 1998. Binding of an arm repeat protein to the kinase domain of the S-locus receptor kinase. *Proceedings of the National Academy of Sciences, USA* **95**, 382–387.
- Hatakeyama K, Horisaki A, Niikura S, Narusaka Y, Abe H, Yoshiaki H, Ishida M, Fukuoka H, Matsumoto S.** 2010. Mapping of quantitative trait loci for high level of self-incompatibility in *Brassica rapa* L. *Genome* **53**, 257–265.
- Hepler PK, Winship LJ.** 2010. Calcium at the cell wall–cytoplasm interface. *Journal of Integrative Plant Biology* **52**, 147–160.
- Horisaki A, Niikura S.** 2008. Developmental and environmental factors affecting level of self-incompatibility response in *Brassica rapa* L. *Sexual Plant Reproduction* **21**, 123–132.
- Hyun JY, Gothandam KM, Baek NK, Wang G, Chung YY.** 2007. Dominance relationship between two self-incompatible *Brassica campestris* haplotypes in response to CO₂ gas. *Journal of Plant Biology* **50**, 161–166.
- Indriolo E, Tharmapalan P, Wright SI, Goring DR.** 2012. The *ARC1* E3 ligase gene is frequently deleted in self-compatible Brassicaceae species and has a conserved role in *Arabidopsis lyrata* self-pollen rejection. *The Plant Cell* **24**, 4607–4620.
- Iwano M, Wada M, Morita Y, Shiba H, Takayama S, Isoga A.** 1999. X-ray microanalysis of papillar cells and pollen grains in the pollination process in *Brassica* using a variable-pressure scanning electron microscope. *Journal of Electron Microscopy* **48**, 909–917.
- Kakita M, Murase K, Iwano M, Matsumoto T, Watanabe M, Shiba H, Isogai A, Takayama S.** 2007. Two distinct forms of M-locus protein kinase localize to the plasma membrane and interact directly with S-locus receptor kinase to transduce self-incompatibility signalling in *Brassica rapa*. *The Plant Cell* **19**, 3961–3973.
- Kitashiba H, Liu P, Nishio T, Nasrallah JB, Nasrallah ME.** 2011. Functional test of *Brassica* self-incompatibility modifiers in *Arabidopsis thaliana*. *Proceedings of the National Academy of Sciences, USA* **108**, 16173–16178.
- Kosambi DD.** 1944. The estimation of map distance from recombination values. *Annals of Eugenics* **12**, 172–175.
- Lee SH, Hong MY, Kim S, Lee JS, Kim BD, Min BH, Baek NK, Chung YY.** 2001. Controlling self-incompatibility by CO₂ gas treatment in *Brassica campestris*: structural alteration of papillae cell and differential gene expression by increased CO₂ gas. *Molecules and Cells* **11**, 186–191.
- Lowe AJ, Moule C, Trick M, Edwards KJ.** 2004. Efficient large-scale development of microsatellites for marker and mapping applications in *Brassica* crop species. *Theoretical and Applied Genetics* **108**, 1103–1112.
- Matsubara S.** 1980. Overcoming self-incompatibility in *Raphanus sativus* L. with high temperature. *Journal of the American Society for Horticultural Science* **105**, 842–846.
- Monterio AA, Gabelman WH.** 1988. Use of sodium chloride solution to overcome self-incompatibility in *Brassica campestris*. *HortScience* **23**, 876–877.
- Murase K, Shiba H, Iwano M, Che FS, Watanabe M, Isogai A, Takayama S.** 2004. A membrane-anchored protein kinase involved in *Brassica* self-incompatibility signaling. *Science* **303**, 1516–1519.
- Murray HG, Thompson WF.** 1980. Rapid isolation of high molecular weight DNA. *Nucleic Acids Research* **8**, 4321–4325.
- Nakanishi T, Esashi Y, Hinata K.** 1969. Control of self-incompatibility by CO₂ gas in *Brassica*. *Plant and Cell Physiology* **10**, 925–927.
- Nakanishi T, Hinata K.** 1973. An effective time for CO₂ gas treatment in overcoming self-incompatibility in *Brassica*. *Plant and Cell Physiology* **14**, 873–879.
- Nasrallah JB, Kao TH, Chen CH, Goldberg ML, Nasrallah ME.** 1987. Amino acid sequence of glycoproteins encoded by three alleles of the S locus of *Brassica oleracea*. *Nature* **326**, 617–619.
- Niikura S, Matsuura S.** 2000. Genetic analysis of the reaction level of self-incompatibility to a 4% CO₂ gas treatment in the radish (*Raphanus sativus* L.). *Theoretical and Applied Genetics* **101**, 1189–1193.
- Nishio T, Kusaba M, Watanabe M, Hinata K.** 1996. Registration of S alleles in *Brassica campestris* L. by the restriction fragment sizes of SLGs. *Theoretical and Applied Genetics* **92**, 388–394.
- Obayashi T, Kinoshita K, Nakai K, Shibaoka M, Hayashi S, Saeki M, Shibata D, Saito K, Ohta H.** 2007. ATTED-II: a database of co-expressed genes and cis elements for identifying co-regulated gene groups in *Arabidopsis*. *Nucleic Acids Research* **35**, D863–D869.
- Ockendon DJ.** 1978. Effects of hexan and humidity on self-incompatibility in *Brassica oleracea*. *Theoretical and Applied Genetics* **52**, 113–117.
- Okazaki K, Hinata K.** 1987. Repressing the expression of self-incompatibility in crucifers by short-term high temperature treatment. *Theoretical and Applied Genetics* **73**, 496–500.
- Paran I, Zamir D.** 2003. Quantitative traits in plants: beyond the QTL. *Trends in Genetics* **19**, 303–306.
- Ramchiary N, Nguyen VD, Li X, Hong CP, Dhandapani V, Choi SR, Yu G, Piao ZY, Lim YP.** 2011. Genic microsatellite markers in *Brassica rapa*: development, characterization, mapping, and their utility in other cultivated and wild *Brassica* relatives. *DNA Research* **18**, 305–320.
- Samuel MA, Chong YT, Haasen KE, Aldea-Brydges MG, Stone SL, Goring DR.** 2009. Cellular pathways regulating responses to compatible and self-incompatible pollen in *Brassica* and *Arabidopsis* stigmas intersect at Exo70A1, a putative component of the exocyst complex. *The Plant Cell* **21**, 2655–2671.
- Sarker RH, Elleman CJ, Dickinson HG.** 1988. Control of pollen hydration in *Brassica* requires continued protein synthesis,

and glycosylation is necessary for intraspecific incompatibility. *Proceedings of the National Academy of Sciences, USA* **85**, 4340–4344.

Schopfer CR, Nasrallah ME, Nasrallah JB. 1999. The male determinant of self-incompatibility in *Brassica*. *Science* **286**, 1405–1412.

Schranz ME, Lysak MA, Mitchell-Olds T. 2006. The ABC's of comparative genomics in the Brassicaceae: building blocks of crucifer genomes. *Trends in Plant Science* **11**, 535–542.

Silva NF, Stone SL, Christie LN, Sulaman W, Nazarian KA, Burnett LA, Arnoldo MA, Rothstein SJ, Goring DR. 2001. Expression of the S receptor kinase in self-compatible *Brassica napus* cv. Wester leads to the allele-specific rejection of self-incompatible *Brassica napus* pollen. *Molecular Genetics and Genomics* **265**, 552–559.

Stone SL, Anderson EM, Mullen RT, Goring DR. 2003. ARC1 is an E3 ubiquitin ligase and promotes the ubiquitination of proteins during the rejection of self-incompatible *Brassica* pollen. *The Plant Cell* **15**, 885–898.

Stone SL, Arnoldo M, Goring DR. 1999. A break down of *Brassica* self-incompatibility in ARC1 antisense transgenic plants. *Science* **286**, 1729–1731.

Suwabe K, Iketani H, Nunome T, Kage T, Hirai M. 2002. Isolation and characterization of microsatellites in *Brassica rapa* L. *Theoretical and Applied Genetics* **104**, 1092–1098.

Suwabe K, Iketani H, Nunome T, Ohyama A, Hirai M, Fukuoka H. 2004. Characteristics of microsatellites in *Brassica rapa* genome and their potential utilization for comparative genomics in Cruciferae. *Breeding Science* **54**, 85–90.

Suwabe K, Morgan C, Bancroft I. 2008. Integration of *Brassica* A genome genetic linkage map between *Brassica napus* and *B. rapa*. *Genome* **51**, 169–176.

Suwabe K, Tsukazaki H, Iketani H, Hatakeyama K, Kondo M, Fujimura M, Nunome T, Fukuoka H, Hirai M, Matsumoto S.

2006. Simple sequence repeat-based comparative genomics between *Brassica rapa* and *Arabidopsis thaliana*: the genetic origin of clubroot resistance. *Genetics* **173**, 309–319.

Takasaki T, Hatakeyama K, Suzuki G, Watanabe M, Isogai A, Hinata K. 2000. The S receptor kinase determines self-incompatibility in *Brassica stigma*. *Nature* **403**, 913–916.

Takayama S, Isogai A, Tsunemoto C, Ueda Y, Hinata K, Okazaki K, Suzuki A. 1987. Sequences of S-glycoproteins, products of the *Brassica campestris* self-incompatibility locus. *Nature* **326**, 102–104.

Takayama S, Shiba H, Iwano M, Shimosato H, Che FS, Kai N, Watanabe M, Suzuki G, Hinata K, Isogai A. 2000. The pollen determinant of self-incompatibility in *Brassica campestris*. *Proceedings of the National Academy of Sciences, USA* **97**, 1920–1925.

Takayama S, Shimosato H, Shiba H, Funato M, Che FS, Watanabe M, Iwano M, Isogai A. 2001. Direct ligand–receptor complex interaction controls *Brassica* self-incompatibility. *Nature* **413**, 534–538.

Tatebe T. 1968. Studies on the physiological mechanism of self-incompatibility in Japanese radish. II. Breakdown of self-incompatibility by chemical treatments. *Journal of the Japanese Society for Horticultural Science* **37**, 43–46.

Tao G, Yang R. 1986. Use of CO₂ and salt solution to overcome self-incompatibility of Chinese cabbage (*B. campestris* ssp. *pekinensis*). *Eucarpia Cruciferae Newsletter* **11**, 75–76.

Upton G, Cook I. 1996. *Understanding statistics*. Oxford: Oxford University Press.

Van Ooijen JW. 2006. JoinMap[®] 4, software for the calculation of genetic linkage maps in experimental populations. Wageningen, The Netherlands: Kyazma BV.

Van Ooijen JW. 2009. MapQTL[®] 4, software for the mapping of quantitative trait loci in experimental populations of diploid species. Wageningen, The Netherlands: Kyazma BV.